JOURNAL OF GUIDANCE, CONTROL, AND DYNAMICS
Vol. 34, No. 4, July–August 2011

Stability Properties and Cross-Coupling Performance of the Control Allocation Scheme CAPIO

Yıldıray Yıldız*
University of California, Santa Cruz, Santa Cruz, California 95064
and
Ilya Kolmanovsky†
University of Michigan, Ann Arbor, Michigan 48109

DOI: 10.2514/1.50310

This paper is concerned with further development of a recently proposed algorithm for control allocation to recover from pilot-induced oscillations (CAPIO). When actuators are rate-saturated due to either an aggressive pilot command, high gain of the flight control system, or some anomaly in the system, the effective time delay in the control loop may increase. This effective time-delay increase manifests itself as a phase shift between the commanded and actual signals and can instigate pilot-induced oscillations. CAPIO reduces the effective time delay by minimizing the phase shift between the commanded and the actual attitude accelerations. Theoretical stability analysis results are presented for a scalar input-signal case. Simulation results for an unstable aircraft with cross-coupling and multiple control channels demonstrate the potential of CAPIO serving as an effective pilot-induced oscillation handler in adverse conditions.

I. Introduction

A PILOT-INDUCED oscillation (PIO) can be described as "sustained or uncontrollable oscillations resulting from efforts of the pilot to control the aircraft" [1,2] or as an "inadvertent, sustained aircraft oscillation which is the consequence of an abnormal joint enterprise between the aircraft and the pilot" [3]. The main commonality between various definitions is that there is an undesired, sustained oscillation due to a pilot-aircraft dynamic coupling and interaction. There are several possible instigators of PIOs such as rate-saturated actuators, high-gain pilot/controller, system time delays and phase lags. In [4], a technique for control allocation to recover from pilot-induced oscillations (CAPIO) due to actuator rate saturation was proposed by the authors. In this paper, a comparison between conventional control allocation and CAPIO is given in the case of a PIO event when the aircraft has inertial cross-coupling. Moreover, stability analysis is provided for systems with CAPIO in a single-input case.

Actuator rate saturation is a frequently observed phenomenon during PIO events that has led to several crashes. A comprehensive overview of the connections between rate limiting and PIO is given by Klyde and Mitchell [5]. Figure 1 presents a basic model for a rate-limited actuator [5], where u is the input command to the actuator and δ is the actual actuator deflection. Figure 2 [5–7] shows time evolutions of input–output signals of such a rate-saturated actuator, where $u_c = u$ represents the pilot command. Gain reduction and an increase in effective time delay are two detrimental results of rate saturation, as seen from this figure.

There are several successful approaches in the literature that address eliminating the effective time delay. Differentiate–limit–integrate (DLI) [8–12] is one of the approaches that is implemented using a software rate limiter as shown in Fig. 3, where the software limiter is placed between the command signal and the input signal to the actuator. This method eliminates the effective time delay introduced by the rate saturation as seen in Fig. 4 and hence the onset of a PIO can be avoided. It has several deficiencies, however, such as introduction of a bias and susceptibility to noise. These deficiencies can be addressed by using techniques in [9–12].

There are also other methods for dealing with the effective time delay based on manipulating the input signal. These methods include nonlinear adaptive filters to attenuate the stick gain [13] and phase-compensating filters [14–16].

To the best of authors' knowledge, almost all of the previously reported successful implementation results of PIO mitigation algorithms were for single-input/single-output (SISO) systems without any redundant actuators. Consider the closed-loop flight control structure in Fig. 5, where the pilot is also in the loop. In this configuration, the pilot task may be to track an altitude reference r, by getting altitude measurement feedback y, and making necessary corrections via a pilot stick that gives pitch rate commands u_c as a reference to the inner-loop flight controller. The inner-loop controller may also be responding to roll and yaw rate commands at the same time. So, the pilot command u_c can be a vector with three components. The controller then calculates the necessary attitude accelerations $v \in \Re^3$ and then the control allocator allocates the available actuators $u \in \Re^m$, $m > 3$, to achieve these desired accelerations while possibly satisfying constraints and secondary objectives like drag minimization. In this scenario, it is not obvious where and how to use the DLI software limiter. An extension of the DLI method to multi-input/multi-output (MIMO) case was given by Hess and Snell [9]; however, the authors had to use ganged actuators for successful implementation. Ganging of the actuators prevents the use of redundant actuators for secondary objectives like drag minimization or reconfiguration after a failure. In addition, ganging becomes more cumbersome as the number of actuators increases [17] and it can significantly degrade the response.

It is noted that Durham and Bordignon [18] extended the direct control allocation scheme to make it easier to implement for the case of rate-limited actuators and consequently ended up with a moment-rate allocation scheme. Although there is no implementation result showing a PIO prevention example in that study, their control

Presented as Paper 2010-3474 at the AIAA Infotech@Aerospace 2010, Atlanta, GA, 20–22 April 2010; received 12 April 2010; revision received 19 January 2011; accepted for publication 19 January 2011.

*Associate Scientist, NASA Ames Research Center, Mail Stop 269-1, Moffett Field, CA 94035; yildiray.yildiz@nasa.gov. Member AIAA.

†Professor, Department of Aerospace Engineering; ilya@umich.edu. Member AIAA.

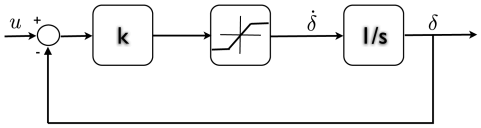

Fig. 1 Actuator model with rate saturation.

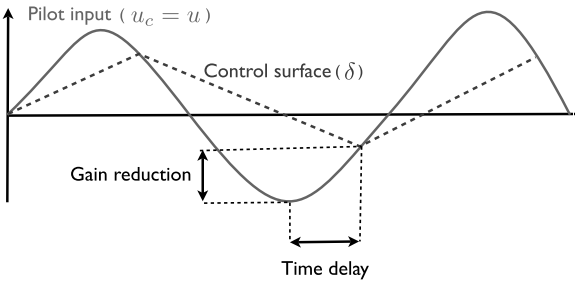

Fig. 2 Input u and output δ of a rate-saturated actuator.

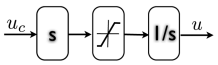

Fig. 3 Software rate limiter.

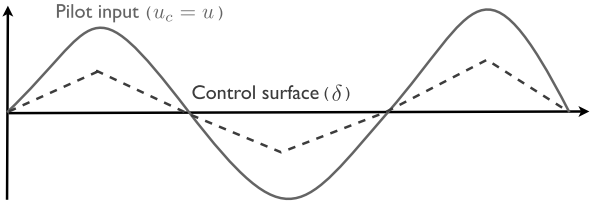

Fig. 4 Input u_c and output δ of a rate-saturated actuator with a preceding software rate limiter.

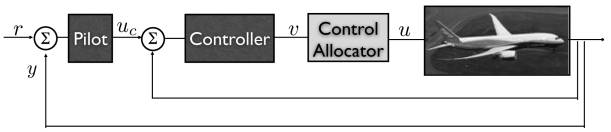

Fig. 5 Overall SISO system structure.

allocation scheme has a potential to handle PIOs despite being more complicated than CAPIO. In particular, the technique in [18] needs the calculation of a moment-rate set that can complicate the computations.

The control allocation method CAPIO, previously proposed by the authors in [4], is suitable for MIMO systems in the presence of redundant actuators. The main idea behind CAPIO is to minimize the phase lag introduced into the system due to rate saturation by minimizing the error between the time derivatives of desired and actual total control effort vectors as well as minimizing the error between them, using constrained optimization techniques. To achieve this goal, for example in a SISO case, one needs to minimize the phase lag between the pilot input and the control surface deflection. On the other hand, in a MIMO case, where there are multiple inputs and outputs, one needs to pinpoint where exactly the phase lag is being introduced into the system. For example, in a scenario where the flight control system produces the desired rate accelerations and a control allocator distributes these commands to redundant actuators using some predefined optimization routine, it makes more sense to minimize the phase lag between the desired and achieved accelerations than concentrating on individual actuator signals. It is noted that merely having a control allocation scheme that takes into account the rate limits of the actuators as constraints cannot prevent phase shift between the desired and achieved accelerations when saturation is unavoidable, and thus may not be able to handle a PIO situation. It was shown in [4], where PIOs were not prevented with conventional control allocation techniques, that the onset of these PIOs could be prevented using CAPIO.

In this paper, new results are presented for the case in which the aircraft is assumed to have inertial cross-coupling. Cross-coupling between the lateral and longitudinal dynamics of aircraft becomes dominant in cases in which the weight is concentrated along the fuselage as the aircraft's wings become thinner and shorter, causing a shift of weight [19]. A similar effect can also be observed in damaged aircraft where the weight shift may occur, for instance, as a result of a more than 25% wing loss [20]. For a cross-coupled aircraft, a PIO becomes more dangerous since an onset of a PIO in one axis can affect other axes, resulting in a catastrophic failure. To the best of the authors' knowledge, no PIO prevention technique was tested for these cases. It is shown in this paper that CAPIO has the potential to help the aircraft recover from PIOs in the presence of cross-coupling. Moreover, it is shown that a scalar closed-loop system that is stable neglecting the rate limiting elements remains stable in the presence of rate limiting elements if CAPIO is used as the control allocator. These stability analysis results can be extended to MIMO systems.

The organization of this paper is as follows. In Sec. II, flight control of an aircraft with inertial cross-coupling is considered. A PIO event is created using a high-gain pilot model and conventional control allocators and CAPIO are compared in terms of their ability to handle the PIO situation. In Sec. III, the stability analysis is given. Finally, in Sec. IV, the main conclusions are summarized.

II. Flight Control of an Aircraft with Inertial Cross-Coupling

To show the advantages of CAPIO, a flight control example using a simplified [21] ADMIRE[‡] model [22] is used with some modifications to simulate inertial cross-coupling. This model includes redundant actuators that make the DLI method hard to apply if one does not want to gang the actuators.

The linearized aircraft model at Mach 0.22, altitude of 3000 m is given by

$$
\begin{aligned}
x &= [\alpha \quad \beta \quad p \quad q \quad r]^T - x_{\text{lin}} \\
y &= Cx = [p \quad q \quad r]^T - y_{\text{lin}} \\
\delta &= [\delta_c \quad \delta_{\text{re}} \quad \delta_{\text{le}} \quad \delta_r]^T - \delta_{\text{lin}} \\
u &= [u_c \quad u_{\text{re}} \quad u_{\text{le}} \quad u_r]^T - u_{\text{lin}} \\
&\times \begin{bmatrix} \dot{x} \\ \dot{\delta} \end{bmatrix} = \begin{bmatrix} A & B_x \\ 0 & -B_\delta \end{bmatrix} \begin{bmatrix} x \\ \delta \end{bmatrix} + \begin{bmatrix} 0 \\ B_\delta \end{bmatrix} u
\end{aligned} \tag{1}
$$

where α, β, p, q, and r are the angle of attack, sideslip angle, roll rate, pitch rate and yaw rate, respectively. The variables δ and u represent the actual and the commanded control surface deflections, respectively. The aircraft control surfaces are canard wings, right and left elevons, and the rudder; $(.)_{\text{lin}}$ refers to values at the operating point where the linearization was performed. The actuators have the following position and rate limits (in rad and rad/s, respectively):

$$
\begin{aligned}
&\delta_c \in [-55, 25] \times \frac{\pi}{180} \\
&\delta_{\text{re}}, \delta_{\text{le}}, \delta_r \in [-30, 30] \times \frac{\pi}{180} \quad \dot{\delta}_c, \dot{\delta}_{\text{re}}, \dot{\delta}_{\text{le}}, \dot{\delta}_r \in [-70, 70] \times \frac{\pi}{180}
\end{aligned} \tag{2}
$$

and have first-order dynamics with a time constant of 0.05 s. It is noted that the position limits in Eq. (2) are the same as those given by Harkegård and Glad [21] and the rate limits are imposed to illustrate CAPIO properties.

[‡]Aerodata Model in Research Environment (ADMIRE), version 3.4h, available online at www.foi.se/admire [retrieved 2011].

To make this model suitable for control allocation implementation, the actuator dynamics are neglected and the control surfaces are viewed as pure moment generators with their influence on $\dot{\alpha}$ and $\dot{\beta}$ neglected. It is noted that the actuator dynamics are present during the simulations; i.e., they are neglected only during the control allocation algorithm derivation. (For an example of where the actuator dynamics are included in the control allocation problem, see [23].) These assumptions lead to the following approximate model:

$$\dot{x} = Ax + B_u u = Ax + B_v v, \qquad v = Bu \tag{3}$$

where

$$B_u = B_v B, \qquad B_v = \begin{bmatrix} 0_{2\times 3} \\ I_{3\times 3} \end{bmatrix}$$

$$A = \begin{bmatrix} -0.5432 & 0.0137 & 0 & 0.9778 & 0 \\ 0 & -0.1179 & 0.2215 & 0 & -0.9661 \\ 0 & -10.5128 & -0.9967 & 0 & 0.6176 \\ 2.6221 & -0.0030 & 0 & -0.5057 & 0 \\ 0 & 0.7075 & -0.0939 & 0 & -0.2127 \end{bmatrix}$$

$$B = \begin{bmatrix} 0 & -4.2423 & 4.2423 & 1.4871 \\ 1.6532 & -1.2735 & -1.2735 & 0.0024 \\ 0 & -0.2805 & 0.2805 & -0.8823 \end{bmatrix}$$

The virtual (total) control effort, v, consists of the angular accelerations in roll, pitch, and yaw. To simulate the effects of inertial cross-coupling, A matrix was modified so that a change in pitch angular velocity creates a moment in roll and yaw axes:

$$A = \begin{bmatrix} -0.5432 & 0.0137 & 0 & 0.9778 & 0 \\ 0 & -0.1179 & 0.2215 & 0 & -0.9661 \\ 0 & -10.5128 & -0.9967 & 1 & 0.6176 \\ 2.6221 & -0.0030 & 0 & -0.5057 & 0 \\ 0 & 0.7075 & -0.0939 & 0.1 & -0.2127 \end{bmatrix} \tag{4}$$

In this flight control example the pilot task is to track a given pitch-angle reference θ_d using a pitch rate q_d stick. In addition, roll rate p and the yaw rate r are to be controlled independently to track their references p_d and r_d. The overall system configuration is given in Fig. 6.

The inner-loop controller is a dynamic inversion controller that uses q_d, p_d and r_d as references and produces the necessary attitude accelerations, $v \in \Re^3$, to track these references. A dynamic inversion control law is designed for v to make the closed-loop dynamics follow a desired reference model:

$$\dot{y}_m = A_m y_m + B_m r_m \tag{5}$$

where $y_m = [\, p_m \quad q_m \quad r_m \,]^T$ represents the desired output vector and $r_m = [\, p_d \quad q_d \quad r_d \,]^T$ is the reference input vector. In this

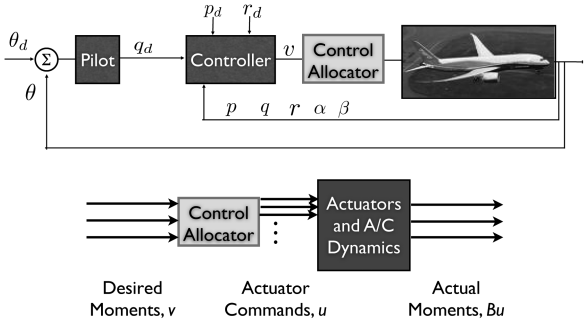

Fig. 6 Overall MIMO system structure.

example, $A_m = -2 \times I_{3\times 3}$ and $B_m = 2 \times I_{3\times 3}$. Reference model tracking can be achieved by inverting the dynamics [17] as

$$v = (CB_v)^{-1}[A_m y + B_m r_m - CAx] \tag{6}$$

The control allocator distributes this total control effort v to individual control surfaces via the actuator commands, $u \in \Re^4$. The control surfaces then produce actual attitude accelerations, Bu, where B is the control input matrix. The pilot is modeled as a pure gain for simplicity.

A. Flight Control with Conventional Control Allocation

The conventional control allocation used in this example minimizes the following objective function:

$$J = \|Bu - v\|_2^2 + \epsilon \|u\|_2^2 \tag{7}$$

subject to $\max(\dot{u}_{\min} T + u^-, u_{\min}) \le u \le \min(\dot{u}_{\max} T + u^-, u_{\max})$, where T is the sampling interval, u^- is the control value at the previous time instant and $u_{\min}, u_{\max}, \dot{u}_{\min}, \dot{u}_{\max}$ denote the magnitude and rate limits, respectively. It is noted that norms, instead of square norms, can be used in the objective function. Note that Eq. (7) is in the form of a typical objective function used in conventional control allocators [17], where the main objective is to minimize the error between the desired and the actual total control efforts. As $\epsilon \to 0$, minimizing Eq. (7) becomes equivalent to minimizing $\|Bu - v\|_2^2$ and picking the solution that gives the minimum control surface deflection, among different solutions. In this example $\epsilon = 10^{-5}$.

Figure 7 presents the simulation result with the conventional control allocation where the pilot receives a step pitch-angle reference at $t = 3$ s and the inner-loop controller receives a pulse yaw rate reference at $t = 0.5$ s and a zero roll rate reference at all times. The pilot is aggressive and has a gain of 4.11. Because of this high gain, the aircraft goes into a divergent PIO in the pitch axis. In addition, inertial cross-coupling causes dangerous oscillations in the roll axis, which finally diverges. Yaw axis also becomes unstable. Canard wings and the ailerons saturate both in position and the rate. The results of saturation can best be observed as a phase shift between the desired pitch acceleration v_2 and the actual pitch acceleration created by the control surfaces Bu_2. This phase shift, or the effective time delay, is almost always observed in PIO events due to actuator saturation.

B. Flight Control with CAPIO

To recover from a PIO event, CAPIO forces the virtual (total) control effort v, to be in phase with the actual control effort Bu produced by the actuators. To achieve this, a derivative error term is added to objective function (7) to obtain the following CAPIO objective function:

$$J' = \|Bu - v\|_2^2 + \|W_d(B\dot{u} - \dot{v})\|_2^2 + \epsilon \|u\|_2^2 \tag{8}$$

where $W_d \in R^{3\times 3}$ represents a weighting matrix on the derivative term. The cost function J' is minimized with respect to u, with $\dot{u} = (u - u^-)/T$, where u^- denotes the value of u at the previous sampling instant. It is noted that with this modified objective function, the control allocator is trying to realize $\dot{v}$ as well as v. Very high values of W_d make the signals, v and Bu, have approximately the same time derivative at all times, which eliminates the phase lag completely but causes a bias. On the other hand, very small values of W_d may not be sufficient for the control allocator to be any different than the conventional one and thus does not prevent PIOs. Therefore, the designer needs to decide on suitable values of W_d that minimize the phase lag and at the same time prevent a bias. As an alternative, the designer can choose to activate W_d, i.e., set it to a constant nonzero matrix, only when PIO is detected, and keep it a 0 matrix at all other times. The latter approach is taken in this paper, assuming that a PIO detection algorithm is available on board of the aircraft. See [24] for examples of PIO detection algorithms. Note that W_d can also be used for axis prioritization. For example, by using a larger value in the corresponding W_d entry, the pitch-axis derivative

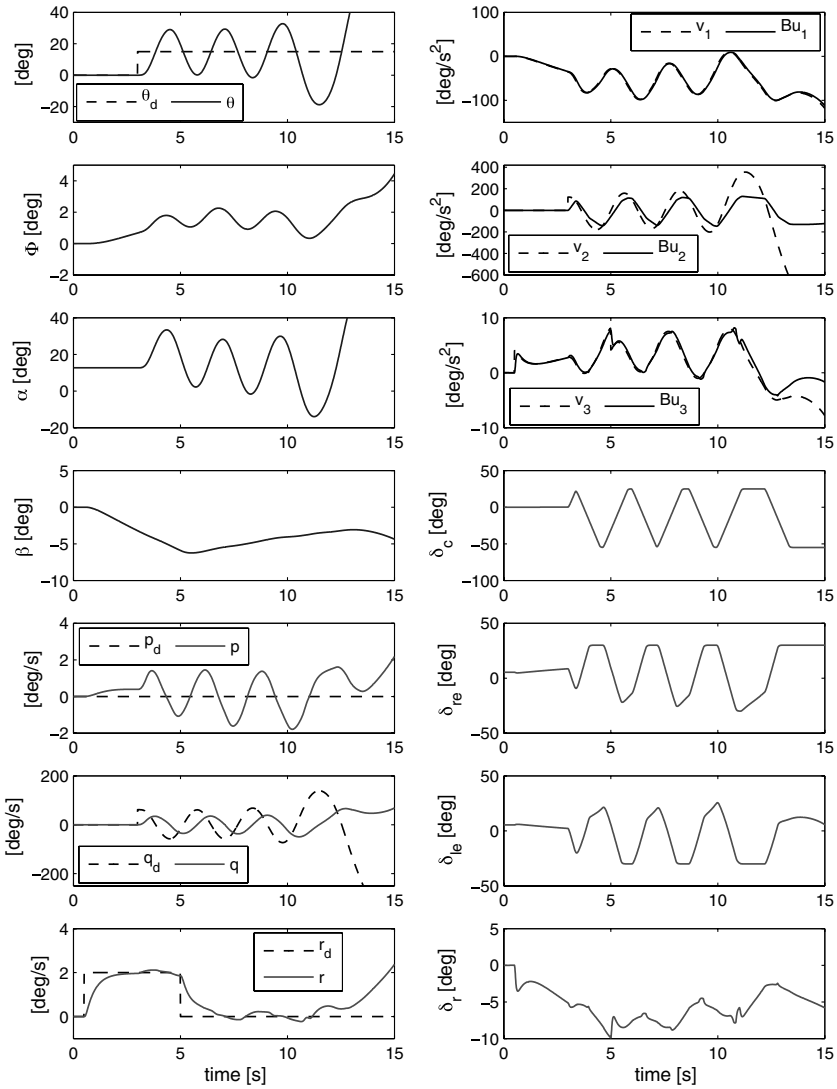

Fig. 7 Pitch and roll angles θ and ϕ, aircraft states x, on the left. Desired (commanded) and actual attitude accelerations v and Bu, and the control surface deflections δ, on the right, when a conventional control allocator is used.

difference minimization can be made the first priority among the axes. Being able to prioritize the axis is important as the control signals are limited. For the simulations in this paper, $W_d = \text{diag}[\,100 \quad 1 \quad 100\,] \times 10^3$ is used.

The objective function (8) needs to be transformed into a form that can be minimized numerically. To achieve this goal, the derivatives in the objective function are approximated as $\dot{u} = (u - u^-)/T$. After some algebra, Eq. (8) can be rewritten as

$$\begin{aligned} J' &= u^T(B^TT^2B + B^TRB + \epsilon I_{4\times 4})u \\ &\quad + 2(-v^TT^2B - u^{-T}B^TRB - \dot{v}^TTRB)u + v^TT^2v \\ &\quad + u^{-T}B^TRBu^- + 2u^{-T}B^TRT\dot{v} + \dot{v}^TT^2R\dot{v} \end{aligned} \tag{9}$$

and it is to be minimized subject to the constraints $\max(\dot{u}_{\min}T + u^-, u_{\min}) \le u \le \min(\dot{u}_{\max}T + u^-, u_{\max})$, where $R = W_d^TW_d$.

Figure 8 presents the simulation result when CAPIO is used as the control allocator. All the settings including the pilot gain are the same as in the previous example with the conventional control allocation. Since CAPIO prevents the effective time-delay introduction, the aircraft is able to recover from the PIO and no dangerous oscillation or divergence is observed in any axis.

To show the difference that CAPIO makes in control effort realization, the pitch-axis accelerations are presented again in Fig. 9 for both cases. It is noted that as soon as the PIO is detected, CAPIO forces the control surfaces to produce accelerations in phase with the commanded accelerations, eliminating the effective time delay due to phase shift. Once the aircraft recovers from PIO, control allocation reverts back to track the commanded acceleration. The result is a recovery from the PIO without any bias formation.

III. Stability Analysis of CAPIO

This section provides insight into CAPIO by presenting two different stability analysis. For the first analysis, a simplifying assumption is made to explain the basic working principles of CAPIO. The second stability analysis is given in a separate subsection where the simplifying assumption is eliminated and a rigorous stability proof is provided.

A closed-loop system is considered where the virtual control input v and real control input u are scalar and it is assumed that the reference input is zero. The resulting system structure is presented in Fig. 10. Consider a plant dynamics represented in state space form and a stabilizing state feedback controller:

$$\dot{x} = Ax + Bu \qquad v = -Kx \tag{10}$$

where $x \in \Re^n$, $A \in \Re^{n\times n}$, $B \in \Re^n$, v is a scalar, and K is such that $(A - BK)$ has only eigenvalues with negative real parts. Note that the plant is not assumed to be open-loop-stable.

It is assumed that W_d is large enough so that CAPIO forces u to behave in the following manner:

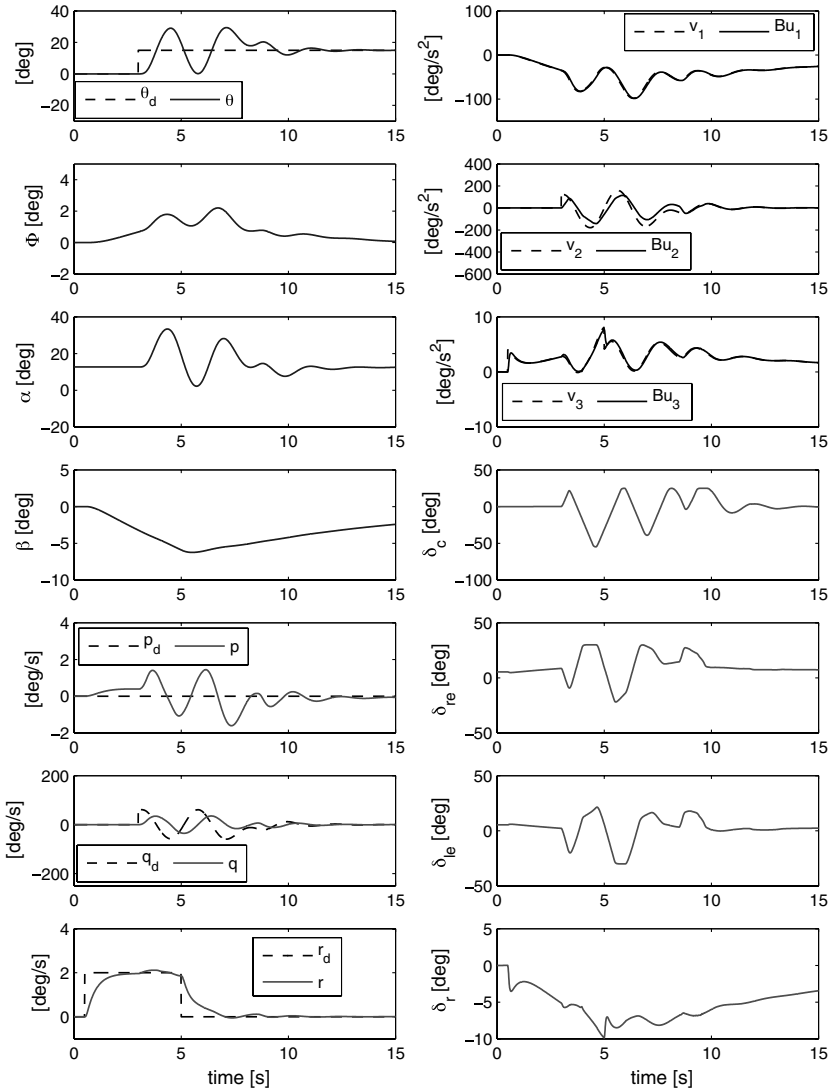

Fig. 8 Pitch angle θ and aircraft states x, on the left. Desired (commanded) and actual attitude accelerations v and Bu, and the control surface deflections δ, on the right, when CAPIO is used.

$$\dot{u} = \text{sign}(\dot{v})l \quad \text{if } |\dot{v}| > l \qquad \dot{u} = \dot{v} \text{ otherwise} \tag{11}$$

where l is the actuator rate limit. It is noted that the second equation in Eq. (11) is due to CAPIO forcing the signals u and v to have the same derivative, i.e., $\dot{u} = \dot{v}$. According to the first equation in Eq. (11), u is trying to follow v as much as possible when actuators are rate-saturated. As soon as the saturation ends, u follows v in a manner that their derivatives become equal. This behavior prevents wind up and the introduction of an effective time delay. When W_d is switched off after the recovery, CAPIO forces u to follow the commanded control input v, thereby preventing bias formation.

It is noted that the system (10) and (11) is a SISO linear system with states (x, u) and saturation at the input v. Its stability may be analyzed using various techniques including Lyapunov functions, describing functions, or circle/Popov criterion.

A. Simple Stability Analysis

For stability analysis it is assumed that there is a PIO event at $t = t_0$ and thus the system is experiencing a sustained oscillation. The commanded control input v is also in a sustained oscillation mode and causing the actuators to rate-saturate. In other words, $\dot{v}$ is oscillating past $\pm l$.

There is no difference between the conventional control allocators and CAPIO when $|\dot{v}| > l$. Both force the actual control signal u to follow the commanded control signal v as closely as possible. However, once $|\dot{v}| \leq l$, CAPIO stabilizes the system for $t \geq t_c$. To show this, consider the closed-loop system behavior in the unsaturated region by employing the second equation in Eq. (11) in the plant dynamics. It is noted that $u = v + d$ for a constant $d = u(t_c) - v(t_c)$ and

$$\dot{x} = Ax + B(v + d) = Ax + B(-Kx + d) = (A - BK)x + Bd \tag{12}$$

Defining $M \equiv A - BK$, the solution to Eq. (12) can be given as

$$x(t) = e^{M(t-t_0)}(x(t_0) + M^{-1}Bd) - M^{-1}Bd \tag{13}$$

Differentiating Eq. (13), it is obtained that

$$\dot{x}(t) = e^{M(t-t_0)}(Mx(t_0) + Bd) \tag{14}$$

Therefore, if $|\dot{v}(t)| \leq l$ for $t \geq t_c$ for some t_c, then

$$\lim_{t\to\infty} x(t) = -M^{-1}Bd, \qquad \lim_{t\to\infty} \dot{x}(t) = 0$$
$$\lim_{t\to\infty} \dot{v}(t) = \lim_{t\to\infty} -K\dot{x}(t) = 0 \tag{15}$$

Hence, $x(t)$ tends to $-M^{-1}Bd$, whenever $|\dot{v}| \leq l$. It is noted that $-M^{-1}Bd$ corresponds to a steady-state error or a bias, which appears until the derivative term is switched off. Once the system recovers from PIO and the derivative term is switched off, CAPIO forces u to follow v and the steady-state error is eliminated. This behavior can be observed in Figs. 8 and 9.

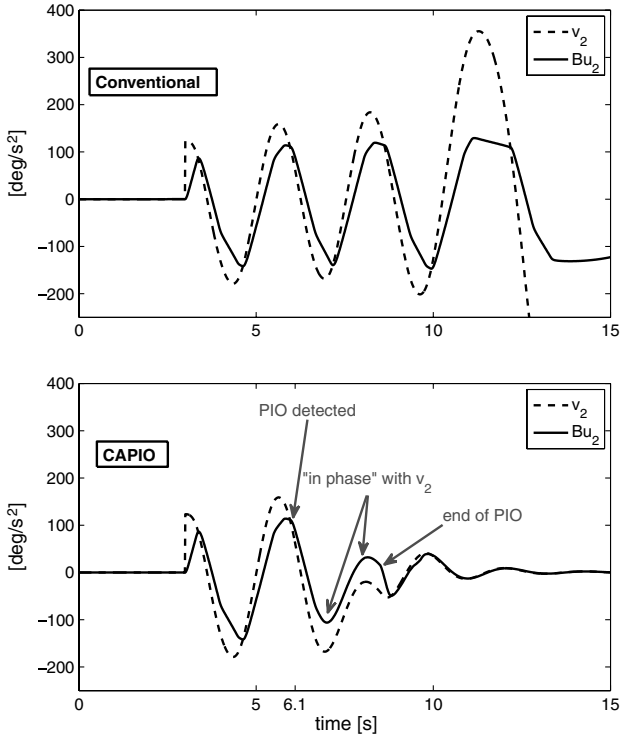

Fig. 9 Commanded and achieved pitch accelerations, Bu_2 and v_2, in the case of a conventional control allocator (top) and CAPIO (bottom).

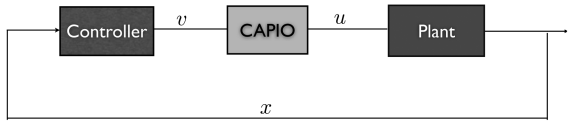

Fig. 10 Closed-loop system with CAPIO.

B. Stability Analysis Using the Popov Criterion

To eliminate the assumption that the system is already in a PIO, the Popov criterion [25] is used to investigate the stability of the overall closed-loop system with CAPIO. Taking the derivative of Eq. (10) and defining $\tilde{x} = \dot{x}$, $\tilde{u} = \dot{u}$, and $\tilde{v} = \dot{v}$, it is obtained that

$$\dot{\tilde{x}} = A\tilde{x} + B\tilde{u} \qquad \tilde{v} = -K\tilde{x} \tag{16}$$

Using the same definitions, Eq. (11) can be rewritten as

$$\tilde{u} = \text{sign}(\tilde{v})l \quad \text{if } |\tilde{v}| > l \qquad \tilde{u} = \tilde{v} \text{ otherwise} \tag{17}$$

Defining $\tilde{u}' = -\tilde{u}$ and $\tilde{v}' = -\tilde{v}$, Eqs. (16) and (17) can be represented as in Fig. 11.

To investigate the stability properties of the closed-loop system given in Fig. 11, the loop transfer function $G(s)$ needs to be known.

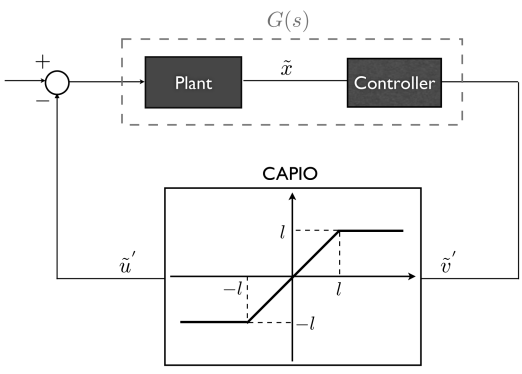

Fig. 11 Closed-loop system with CAPIO, reconfigured.

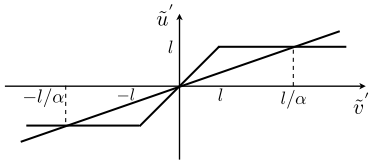

Fig. 12 Sector for CAPIO nonlinearity.

The pitch-angle control system example that was given in [4] will be used where CAPIO was introduced without investigating the closed-loop stability. Consider the short-period dynamics for aircraft given as

$$P(s) = \frac{1.39(s + 0.306)}{s^3 + 0.805s^2 + 1.325s} \tag{18}$$

It is also assumed that the pilot (controller) is a pure gain that has a value of 1.65. Therefore, the loop transfer function is obtained as

$$G(s) = \frac{2.293(s + 0.306)}{s^3 + 0.805s^2 + 1.325s} \tag{19}$$

According to the Popov criterion, to show that the closed-loop system is absolutely stable, the nonlinearity must belong to the sector $[0, k]$ (see [25] chapter 7 for sector definition and Popov criterion) and the following transfer function must be strictly positive real (SPR).

$$ZZ(s) = \frac{1}{k} + (1 + s\gamma)G(s) \tag{20}$$

where $\gamma > 0$ is such that $(1 + \lambda_i\gamma) \neq 0$, for any eigenvalue λ_i of the plant $G(s)$. For $ZZ(s)$ to be SPR, $G(s)$ must be Hurwitz. However, it is known that $G(s)$, given in Eq. (19), is not Hurwitz. To address this issue, first, the domain of $\tilde{v}$ is restricted to $[-l/\alpha, l/\alpha]$ as seen in Fig. 12. With this restriction, CAPIO $\in [\alpha, 1]$ is obtained. The largest sector that the nonlinearity can be accommodated is sought after and therefore it is assumed that CAPIO $\in [\alpha, \beta]$ and the goal is to find the largest β and smallest α that is allowed. To represent the problem in accordance with the Popov criterion requirements, the loop transformation is applied as shown in Fig. 13. After this transformation, the nonlinearity is transformed to CAPIO$_t \in [0, k]$, where $k = \beta - \alpha$. In addition, the transformed linear system becomes

$$G_t(s) = \frac{2.293(s + 0.306)}{s^3 + 0.805s^2 + (1.325 + 2.293\alpha)s + 0.7017\alpha} \tag{21}$$

To show that $ZZ_t(s) = (1/k) + (1 + s\gamma)G_t(s)$ is SPR, it is necessary to prove that

$$\frac{1}{k} + \text{Re}[G_t(j\omega)] - \gamma\omega\text{Im}[G_t(j\omega)] > 0, \quad \forall\ \omega \in [-\infty, \infty] \tag{22}$$

Substituting Eq. (21) into Eq. (22), it is obtained, after some algebra, that

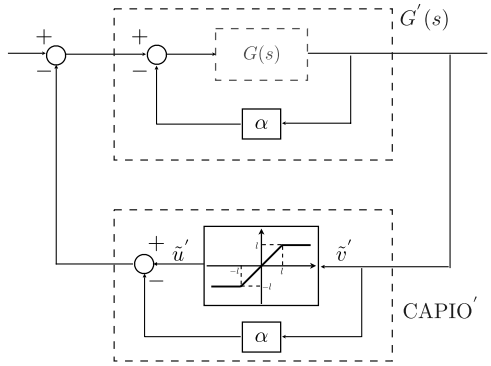

Fig. 13 CAPIO $\in [\alpha, \beta]$ transformed to CAPIO$_t \in [0, \beta - \alpha]$ via loop transformation.

$$\frac{1}{k}+\frac{(1.8459\gamma-2.293)\omega^4+(2.4733+5.2578\alpha+0.9298\gamma)\omega^2+0.4924\alpha}{(0.7017\alpha-0.805\omega^2)^2+(1.325\omega+2.293\alpha\omega-\omega^3)^2}>0 \tag{23}$$

It is clear that for any positive values of k and α and for $\gamma > 1.2422$, Eq. (23) is satisfied. For $k=\infty$, the inequality is satisfied for $\omega \in (-\infty, \infty)$ and

$$\lim_{\omega\to\infty}\frac{\omega^2((1.8459\gamma-2.293)\omega^4+(2.4733+5.2578\alpha+0.9298\gamma)\omega^2+0.4924\alpha)}{(0.7017\alpha-0.805\omega^2)^2+(1.325\omega+2.293\alpha\omega-\omega^3)^2}=1.8459\gamma-2.293>0 \tag{24}$$

Therefore, the system is absolutely stable for all nonlinearities that belongs to the sector $[\alpha, \infty]$. Note that α can be selected arbitrarily small. This means that the system shown in Fig. 11 with CAPIO is absolutely stable, regardless of the rate of the control input.

IV. Conclusions

The proposed control allocation to recover from pilot-induced oscillations (CAPIO) approach was shown through simulations to successfully mitigate multi-axis pilot-induced oscillation (PIO) events in inertially cross-coupled, open-loop unstable aircraft configurations. The computations involved in the implementation of CAPIO reduce to a quadratic programming problem with linear inequality constraints, which is easily solvable and reconfigurable online. Once conditions leading to onset of PIO are removed, CAPIO behavior reduces to that of conventional control allocation. Through the detailed analysis of the single-input/single-output case it was rigorously demonstrated that CAPIO maintains stability in the presence of actuator rate limits. These results provide motivation to proceed to the actual pilot-in-the-loop tests, which will be conducted at NASA.

Acknowledgments

The authors would like to thank to Kalmanje S. Krishnakumar of NASA for his suggestion of testing control allocation to recover from pilot-induced oscillations for inertially cross-coupled aircraft. The authors also wish to acknowledge Diana Acosta of NASA for valuable discussions.

References

[1] Department of Defense Interface Standard,—Flying Qualities of Piloted Aircraft, MIL-STD-1797A, Jan. 1990.

[2] Jeram, G. J., and Prasad, J. V. R., "Tactile Avoidance Cueing For Pilot Induced Oscillation," AIAA Paper 2003-5311, Austin, TX, Aug. 2003.

[3] McRuer, D., "Human Dynamics and Pilot-Induced Oscillations," *Minta Martin Lecture*, Massachusetts Institute of Technology, Cambridge, MA, 1992.

[4] Yildiz, Y., and Kolmanovsky, I. V., "A Control Allocation Technique to Recover from Pilot-Induced Oscillations (CAPIO) due to Actuator Rate Limiting," *Proceedings of the American Control Conference*, IEEE Press, Piscataway, NJ, 2010, pp. 516–523.

[5] Klyde, D. H., and Mitchell, D. G., "Investigating the Role of Rate Limiting In Pilot-Induced Oscillations," AIAA Paper 2003-5463, Aug. 2003.

[6] McRuer, D., Klyde, D. H., and Myers, T. T., "Development of a Comprehensive PIO Theory," AIAA Paper 1996-3433, July 1996.

[7] Klyde, D. H., and Mitchell, D. G., "A PIO Case Study—Lessons Learned Through Analysis," AIAA Paper 2005-5813, Aug. 2005.

[8] Deppe, P., Chalk, C., and Shafer, M., "Flight Evaluation of an Aircraft with Side and Centerstick Controllers and Rate-Limited Ailerons," Advanced Technology Center, Calspan Corp., Final Rept. 8091-2, Buffalo, NY, April 1994.

[9] Hess, R. A., and Snell, S. A., "Flight Control System Design and Rate Saturating Actuators," *Journal of Guidance, Control, and Dynamics*, Vol. 20, No. 1, 1997, pp. 90–96. doi:10.2514/2.3999

[10] Snell, S. A., and Hess, R. A., "Robust Decoupled, Flight Control Design with Rate-Saturating Actuators," *Journal of Guidance, Control, and Dynamics*, Vol. 21, No. 3, 1998, pp. 361–367. doi:10.2514/2.4253

[11] Chapa, M., "A Nonlinear Pre-Filter To Prevent Departure and/or Pilot-Induced Oscillations (PIO) Due To Actuator Rate Limiting," M.S. Thesis, AFIT/GAE/ENY/99M-01, Graduate School of Engineering, Air Force Inst. of Technology, Wright-Patterson AFB, OH, March 1999.

[12] Liebst, B. S., Chapa, M. J., and Leggett, D. B., "Nonlinear Prefilter to Prevent Pilot-Induced Oscillations due to Actuator Rate Limiting," *Journal of Guidance, Control, and Dynamics*, Vol. 25, No. 4, 2002, pp. 740–747. doi:10.2514/2.4941

[13] Smith, J. W., and Edwards, J. W., "Design Of A Nonlinear Adaptive Filter for Suppression of Shuttle Pilot-Induced Oscillation Tendencies," NASA TM-81349, April 1980.

[14] Koper, J., "An Approach for Compensating Actuator Rate Saturation," Naval Air Development Center, Interim Rept. NADC-87120-60, Air Vehicle and Crew systems Technology Department, Warminster, PA, Aug. 1987.

[15] Rundqwist, L., and Hillgren, R., "Phase Compensation of Rate Limiters in JAS 39 Gripen," AIAA Paper 1996-3368, July 1996.

[16] Hanke, D., "Phase Compensation: A Means of Preventing Aircraft-Pilot Coupling Caused by Rate Limitation," DLR, Forschungsbericht, TR 98-15, 1998.

[17] Bodson, M., "Evaluation of Optimization Methods for Control Allocation," AIAA Paper 2001-4223, Aug. 2001.

[18] Durham, W. C., and Bordignon, K. A., "Multiple Control Effector Rate Limiting," *Journal of Guidance, Control, and Dynamics*, Vol. 19, No. 1, 1996, pp. 30–37. doi:10.2514/3.21576

[19] Blakelock, J. H., *Automatic Control of Aircraft and Missiles*, 2nd ed., Wiley, New York, 1991, Chap. 5.

[20] Nguyen, N., Krishnakumar, K., Kaneshige, J., and Nespeca, P., "Dynamics and Adaptive Control for Stability Recovery of Damaged Asymmetric Aircraft," AIAA Paper 2006-6049, Aug. 2006.

[21] Harkegård, O., and Glad, S. T., "Resolving Actuator Redundancy—Optimal Control vs. Control Allocation," *Automatica*, Vol. 41, 2005, pp. 137–144. doi:10.1016/S0005-1098(04)00255-9

[22] Backström, H., "Report on the Usage of the Generic Aerodata Model," Saab Aircraft AB, Linkoping, Sweden, May 1997.

[23] Oppenheimer, M., and Doman, D., "Methods for Compensating for Control Allocator and Actuator Interactions," *Journal of Guidance, Control, and Dynamics*, Vol. 27, No. 5, 2004, pp. 922–927. doi:10.2514/1.7004

[24] Mitchell, D. G., and Arencibia, A. J., "Real-Time Detection of Pilot-Induced Oscillations," AIAA Paper 2004-4700, Aug. 2004.

[25] Khalil, K. H., *Nonlinear Systems*, 3rd ed., Prentice–Hall, Upper Saddle River, NJ, 2002, Chap. 7.